

# Communications

## Printed Ring Slot Antenna for Circular Polarization

Kin-Lu Wong, Chien-Chin Huang, and Wen-Shan Chen

**Abstract**—A new design of a microstrip-line-fed circularly polarized printed ring slot antenna is proposed. Circular polarization (CP) radiation of the proposed design is achieved by introducing proper asymmetry in the ring slot structure and feeding the ring slot using a microstrip line at  $45^\circ$  from the introduced asymmetry. The asymmetry introduced in the proposed design is a meandered-slot section and the proposed CP design can be applied to printed square and annular ring slot antennas. Prototypes of the proposed design have been implemented. Experimental results show that good CP radiation performances are obtained and the 3 dB axial-ratio CP bandwidths obtained for the square and annular ring slot antennas are about 4.3% and 3.5%, respectively.

**Index Terms**—Circular polarization (CP), printed-ring-slot antenna.

### I. INTRODUCTION

With the introduction of some asymmetry in the structure [1] to a single-feed ring microstrip antenna, it is possible to excite two orthogonal degenerate resonant modes for circular polarization radiation (CP). Since the printed-ring-slot antenna is a dual of the ring-microstrip antenna, it is also possible that by introducing some asymmetry to the ring-slot structure, CP radiation of printed-ring-slot antennas can be obtained. Also, since printed-slot antennas usually have a wider-impedance bandwidth than microstrip antennas, the obtained CP bandwidth for a printed-ring-slot antenna can be expected to be greater than that of a ring-microstrip antenna operated in the fundamental mode. This makes the design of circularly polarized printed-ring-slot antennas attractive. However, relatively fewer CP designs using a printed-ring-slot antenna have been available in the open literature. The related designs that have been reported are associated with the method of introducing some symmetric perturbation elements in the annular ring slot structure, such as the use of a pair of notches placed at  $45^\circ$  and  $225^\circ$  from the feed point for achieving CP radiation in the fundamental mode [2] or four notches placed midway between E- and H-planes at  $22.5^\circ$  and  $112.5^\circ$  from the feed point for CP radiation in a higher-order mode [3].

In this paper, we propose a new design of a circularly polarized printed-ring-slot antenna using the method of introducing asymmetry in the slot structure. The proposed asymmetry has a simple structure of a meandered slot section. Some prototypes of the proposed CP design applied to square- and annular-ring-slot antennas have been implemented and experimental results are presented and discussed.

### II. ANTENNA DESIGNS

Fig. 1(a) and (b) show, respectively, the proposed printed square- and annular-ring-slot antennas with a meandered slot section for CP radiation. Both antennas are printed on a microwave substrate of thickness  $h$  and relative permittivity  $\epsilon_r$ . For the square-ring-slot antenna, the outer- and inner-linear dimensions are  $L_1$  and  $L_2$ , respectively, and the slot

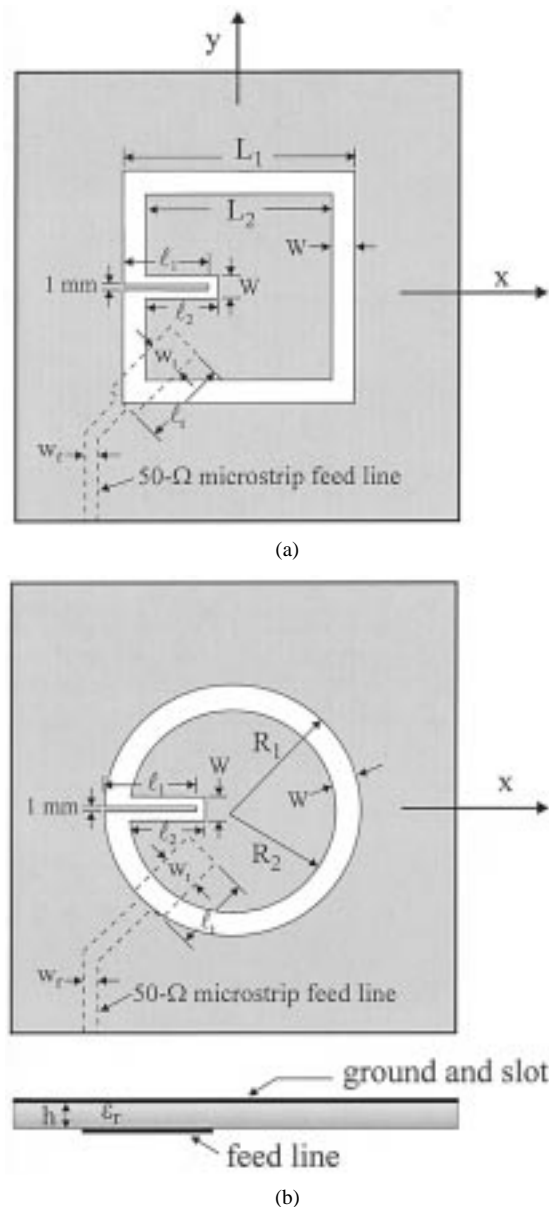


Fig. 1. Configurations of the proposed circularly polarized printed ring slot antenna. (a) Printed square ring slot antenna (antenna A). (b) Printed annular-ring-slot antenna (antenna B).

width is  $W$ . The meandered slot section is placed at the center of one of the slot edges and has a protruded rectangular slot of length  $\ell_2$  and width  $W$  (the width is the same as that of the square ring slot) and a metallic strip of narrow width  $1\text{ mm}$  and length  $\ell_1$ , which is centered in the rectangular slot. Also note that the length  $\ell_1$  is related to  $\ell_2$  with the expression of  $\ell_1 = \ell_2 + 0.5W + 0.5\text{ mm}$  in the proposed design, which results in a uniform slot width  $[\approx 0.5(W - 1\text{ mm})]$  along the meandered slot section. A  $50\text{-}\Omega$  microstrip feed line with a widened tuning stub of length  $\ell_t$  and width  $w_t$  is used to feed the ring slot along the diagonal direction;  $w_t$  is chosen to be about two times  $w_f$  in this study ( $w_f$  is the width of the  $50\text{-}\Omega$  microstrip line). With the widened tuning stub [4], the coupling between the microstrip feed line and the

Manuscript received March 19, 2000; revised December 14, 2000.

The authors are with the Department of Electrical Engineering, National Sun Yat-Sen University, Kaohsiung, Taiwan 804, Republic of China.

Publisher Item Identifier S 0018-926X(02)00767-6.

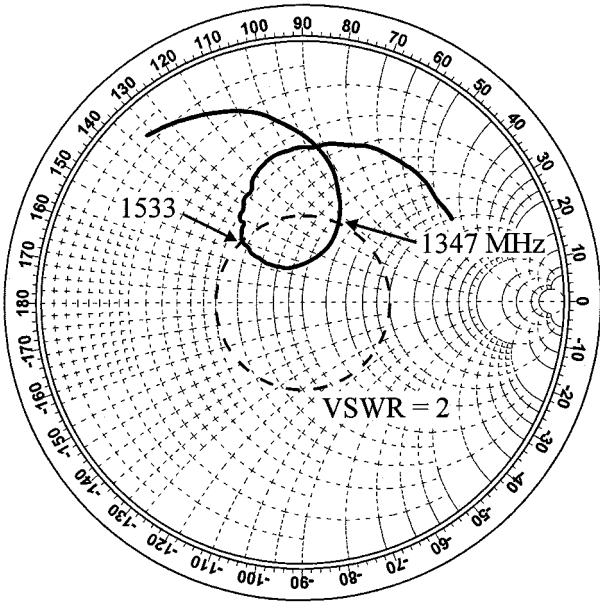


Fig. 2. Measured input impedance on Smith chart for antenna A;  $L_1 = 40$  mm,  $L_2 = 32$  mm,  $W = 4$  mm,  $\ell_1 = 15$  mm,  $\ell_2 = 12.5$  mm,  $\ell_t = 10$  mm,  $w_t = 6$  mm,  $w_f = 3.1$  mm,  $h = 1.6$  mm,  $\epsilon_r = 4.4$ , ground-plane size =  $80 \times 80$  mm.

ring slot can be enhanced and good impedance matching for achieving CP radiation in the proposed design can be easily achieved.

For the design shown in Fig. 1(b), the annular-ring-slot antenna has an outer radius  $R_1$ , an inner radius  $R_2$ , and a slot width  $W$ . The meandered slot section and the microstrip feed line with a widened tuning stub are with the same variables as those in the square-ring-slot antenna in Fig. 1(a). For conventional square- and annular-ring-slot antennas, the fundamental resonant mode occurs at the frequency whose wavelength in the ring slot approximately corresponds to the mean circumference of the ring slot. That is, we have

$$f_a \approx \frac{c}{2(L_1 + L_2)} \times \left( \frac{1 + \epsilon_r}{2\epsilon_r} \right)^{1/2} \quad (1)$$

$$f_b \approx \frac{c}{\pi(R_1 + R_2)} \times \left( \frac{1 + \epsilon_r}{2\epsilon_r} \right)^{1/2} \quad (2)$$

where  $c$  is the speed of light in free space;  $f_a$  and  $f_b$  are, respectively, the fundamental resonant frequencies of the conventional square- and annular-ring-slot antennas;  $2(L_1 + L_2)$  and  $\pi(R_1 + R_2)$  are the mean circumferences of the square- and annular-ring-slot antennas, respectively; the second term in (1) and (2) is the correction factor considering the presence of different dielectric media on the two sides of the slot antenna [5]. In this study, the differences between the measured data and calculated results from (1) and (2) are within 5%.

With the introduced meandered slot section, the symmetry of the ring-slot antenna is perturbed and the fundamental resonant mode can be split into two orthogonal degenerate resonant modes for CP radiation. The optimal value of  $\ell_2$  in this study, is found from many experiments to be about 40% of  $L_2$  (the square ring slot's inner linear dimension) or  $2R_2$  (the annular ring slot's inner diameter). Also note that the design arrangements shown in Fig. 1(a) and (b) radiate a right-hand circularly polarized (RHCP) wave and when the microstrip feed line excites the ring-slot antenna along the other diagonal direction (i.e.,  $90^\circ$  from the feed line shown in the figure), left-hand circularly polarized (LHCP) radiation can be obtained.

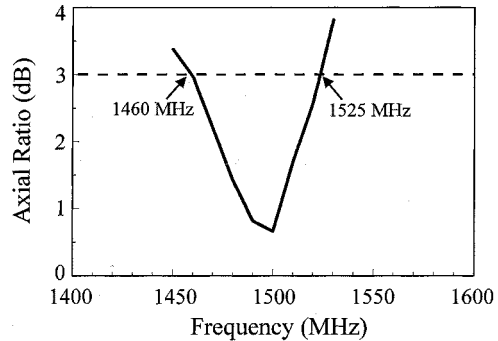


Fig. 3. Measured axial ratio in broadside direction for antenna A; parameters are given in Fig. 2.

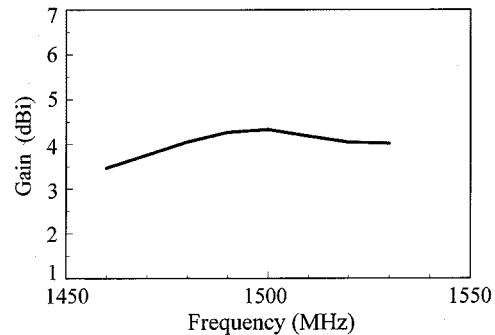


Fig. 4. Measured antenna gain of RHCP in broadside direction for antenna A; parameters are given in Fig. 2.

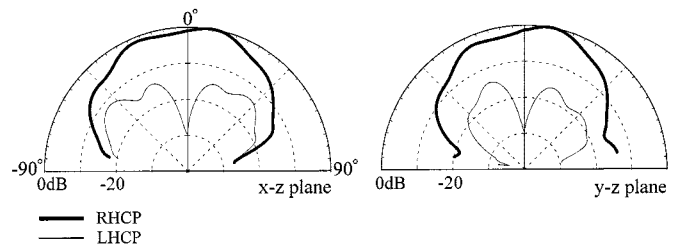


Fig. 5. Measured radiation patterns in two principal planes at 1500 MHz for antenna A; parameters are given in Fig. 2.

### III. EXPERIMENTAL RESULTS AND CONCLUSION

Measured input impedance of a prototype for the proposed square-ring-slot antenna is presented in Fig. 2 and Fig. 3 shows the measured axial ratio. The 3-dB axial-ratio CP bandwidth is observed to be 65 MHz or about 4.3% with respect to the center frequency at 1500 MHz (the center frequency is defined here to be the frequency with minimum axial ratio in the CP bandwidth). It should also be noted that the center frequency is smaller than the fundamental resonant frequency (about 1.7 GHz) of a corresponding conventional ring-slot antenna without the meandered slot section. The measured antenna gain and the radiation patterns at 1.5 GHz are shown in Figs. 4 and 5, respectively. The antenna gain within the CP bandwidth is about 3.5 to 4.3 dBi. Also, a slight asymmetry in the radiation patterns is observed, which is probably owing to the introduced asymmetry (the meandered slot section) in the ring-slot structure.

The proposed design is also applicable to an annular-ring-slot antenna. Fig. 6 shows the measured axial ratio of a constructed prototype. The 3-dB axial-ratio bandwidth is 60 MHz or about 3.5% referenced to the center frequency at 1720 MHz. The obtained center frequency is

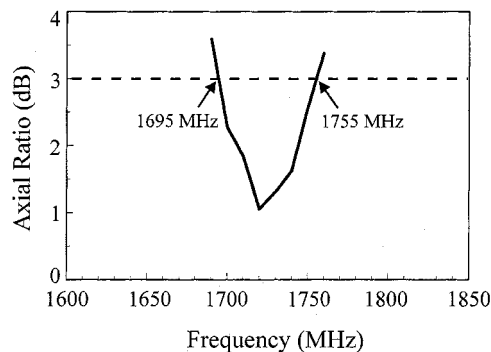


Fig. 6. Measured axial ratio in broadside direction for antenna B;  $R_1 = 20$  mm,  $R_2 = 16$  mm,  $W = 4$  mm,  $\ell_1 = 15$  mm,  $\ell_2 = 12.5$  mm,  $\ell_t = 10$  mm,  $w_t = 6$  mm,  $w_f = 3.1$  mm,  $h = 1.6$  mm,  $\epsilon_r = 4.4$ , ground-plane size =  $80 \times 80$  mm<sup>2</sup>.

also lower than the fundamental resonant frequency (about 2.1 GHz) of a corresponding conventional annular-ring-slot antenna. The measured antenna gain for frequencies within the CP bandwidth is about 3.2 to 3.8 dBi. Finally, it should be noted, that owing to the meandered slot section introduced in the proposed design, the CP radiation occurs at a lowered frequency compared to the fundamental resonant frequency of a corresponding conventional ring-slot antenna, which suggests that reduced ring-slot dimensions can also be obtained for the proposed antenna at a fixed frequency. Also, the obtained CP's center frequency for the proposed ring-slot antenna can be approximately determined from (1) and (2) by modifying the ring slot's mean circumferences to be  $2(L_1 + L_2) + \ell_1 + \ell_2$  and  $\pi(R_1 + R_2) + \ell_1 + \ell_2$ , respectively. In this case, the differences between the measured data and calculated results from (1) and (2) are about 9% and 3%, respectively, for square and annular ring slot antennas.

#### REFERENCES

- [1] K. Chang, *Microwave Ring Circuits and Antennas*, New York: Wiley, 1996.
- [2] K. Hirose and H. Nakano, "Dual-loop slot antenna with simple feed," *Electron. Lett.*, vol. 25, pp. 1218–1219, 1989.
- [3] J. C. Batchelor and R. J. Langley, "Microstrip annular ring slot antennas for mobile applications," *Electron. Lett.*, vol. 32, pp. 1635–1636, 1996.
- [4] S. D. Targonski, R. B. Waterhouse, and D. M. Pozar, "Design of wide-band aperture-stacked patch microstrip antennas," *IEEE Trans. Antennas Propagat.*, vol. 46, pp. 1245–1251, 1998.
- [5] J. S. Rao and B. N. Das, "Impedance characteristics of transverse slots in the ground plane of a stripline," *Inst. Elec. Eng. Proc.*, vol. 125, pp. 29–32, 1978.

### Efficient Calculation of Self/Mutual Impedances in MoM Analysis of a Monopole in Free Space

K. W. Leung

**Abstract**—This paper presents an analysis of a monopole in free space. The result is given in a concise form that facilitates the numerical

Manuscript received September 29, 1999; revised March 2001. This work is supported by a RGC Earmarked Research Grant, No. 9040433.

The author is with the Department of Electronic Engineering, City University of Hong Kong, Kowloon, Hong Kong (e-mail: eekleung@cityu.edu.hk).

Publisher Item Identifier S 0018-926X(02)00770-6.

programming. Moreover, the calculation involves no numerical integration and, thus, the computation is extremely fast.

**Index Terms**—Moment methods (MoM), monopole antennas.

#### I. INTRODUCTION

The dipole antenna is one of the most popular antennas. Tremendous effort has been devoted to analyze the dipole antenna rigorously [1]–[3] and a concise formula has been developed for its efficient numerical implementation [4]. The problem of a monopole protruding from an infinite ground plane is also frequently found. This problem can be solved easily using the dipole result by invoking the image theory. The dipole result, however, cannot be applied for the problem of a monopole in free space. This problem is found when the monopole is mounted on a finite-size object instead of the infinite-ground plane. For example, Tesche *et al.* encountered this problem in solving the problem of a monopole located on a spherical vehicle [5], [6], where the particular solution [7] is in fact the free-space monopole problem. Tesche *et al.* used the moment method (MoM) and employed a pulse expansion with a delta function testing basis set. The choice of the expansion and testing functions was merely to minimize the calculation of the homogeneous solution that accounts for the presence of the spherical body [7]. To speed the MoM convergence for current distributions, however, the piecewise sinusoidal (PWS) basis function and the Galerkin's procedure are usually used [4]. In this paper, a formulation that employs the PWS basis and testing functions is carried out for a monopole in free space. A concise result, analogous to the dipole one [4] is presented for the first time for the evaluation of the self/mutual impedances. Since the result involves no numerical integration, it is computationally very efficient.

#### II. THEORY

Fig. 1(a) shows a monopole of length  $l$  and radius  $y_1$ , which is excited at  $z = 0$ . The negative voltage is on the actual object to which the monopole is attached and is omitted from the figure. It is assumed that the current flows on the  $z$ -axis and its field reacts with a current on the monopole surface to give the self/mutual impedances. This approximation leads to the so-called reduced kernel [7], which is widely accepted and used in the literature [8]. Employing the MoM, the monopole current is expanded as  $I(z) = \sum_{q=1}^N I_q f_q(z)$  where  $I_q$  is the unknown expansion coefficient and  $f_q(z)$  is a normalized PWS function given by  $f_q(z) = [\sin k(d - |z - z_q|)] / \sin kd$  for  $|z - z_q| < d$  and  $f_q(z) = 0$  otherwise, with  $z_q = (q - 1)d$  and  $d = l/N$ . The normalized PWS expansion modes are shown in Fig. 1(b). Note that the half PWS current [9] is used for the first ( $q = 1$ ) current mode. Because of this current mode, the current expansion is asymmetric, substantially increasing the complexity of the analysis. To begin with the self impedance  $Z_{11}$  for the first current mode is determined. Following the procedure given in [10], the  $H_\phi$  component due to the half PWS current is found

$$H_\phi = \frac{j}{4\pi \sin kd} \cdot \frac{1}{y_1} \left( e^{-jkR_1} - \cos kd e^{-jkr} - j \frac{z}{r} \sin kd e^{-jkr} \right) \quad (1)$$

where  $R_1 = \sqrt{(z - d)^2 + y_1^2}$  and  $r = \sqrt{z^2 + y_1^2}$ . It should be mentioned that the third term inside the bracket,  $-j(z/r) \sin kd e^{-jkr}$ , arises from the asymmetry of the current mode and is not present in the dipole case. From (1), the  $z$ -directed  $E$ -field is found by using

## 射频和天线设计培训课程推荐

易迪拓培训([www.edatop.com](http://www.edatop.com))由数名来自于研发第一线的资深工程师发起成立,致力并专注于微波、射频、天线设计研发人才的培养;我们于 2006 年整合合并微波 EDA 网([www.mweda.com](http://www.mweda.com)),现已发展成为国内最大的微波射频和天线设计人才培养基地,成功推出多套微波射频以及天线设计经典培训课程和 ADS、HFSS 等专业软件使用培训课程,广受客户好评;并先后与人民邮电出版社、电子工业出版社合作出版了多本专业图书,帮助数万名工程师提升了专业技术能力。客户遍布中兴通讯、研通高频、埃威航电、国人通信等多家国内知名公司,以及台湾工业技术研究院、永业科技、全一电子等多家台湾地区企业。

易迪拓培训课程列表: <http://www.edatop.com/peixun/rfe/129.html>



### 射频工程师养成培训课程套装

该套装精选了射频专业基础培训课程、射频仿真设计培训课程和射频电路测量培训课程三个类别共 30 门视频培训课程和 3 本图书教材;旨在引领学员全面学习一个射频工程师需要熟悉、理解和掌握的专业知识和研发设计能力。通过套装的学习,能够让学员完全达到和胜任一个合格的射频工程师的要求...

课程网址: <http://www.edatop.com/peixun/rfe/110.html>

### ADS 学习培训课程套装

该套装是迄今国内最全面、最权威的 ADS 培训教程,共包含 10 门 ADS 学习培训课程。课程是由具有多年 ADS 使用经验的微波射频与通信系统设计领域资深专家讲解,并多结合设计实例,由浅入深、详细而又全面地讲解了 ADS 在微波射频电路设计、通信系统设计和电磁仿真设计方面的内容。能让您在最短的时间内学会使用 ADS,迅速提升个人技术能力,把 ADS 真正应用到实际研发工作中去,成为 ADS 设计专家...



课程网址: <http://www.edatop.com/peixun/ads/13.html>



### HFSS 学习培训课程套装

该套课程套装包含了本站全部 HFSS 培训课程,是迄今国内最全面、最专业的 HFSS 培训教程套装,可以帮助您从零开始,全面深入学习 HFSS 的各项功能和在多个方面的工程应用。购买套装,更可超值赠送 3 个月免费学习答疑,随时解答您学习过程中遇到的棘手问题,让您的 HFSS 学习更加轻松顺畅...

课程网址: <http://www.edatop.com/peixun/hfss/11.html>

## CST 学习培训课程套装

该培训套装由易迪拓培训联合微波 EDA 网共同推出,是最全面、系统、专业的 CST 微波工作室培训课程套装,所有课程都由经验丰富的专家授课,视频教学,可以帮助您从零开始,全面系统地学习 CST 微波工作的各项功能及其在微波射频、天线设计等领域的设计应用。且购买该套装,还可超值赠送 3 个月免费学习答疑...

课程网址: <http://www.edatop.com/peixun/cst/24.html>



## HFSS 天线设计培训课程套装

套装包含 6 门视频课程和 1 本图书,课程从基础讲起,内容由浅入深,理论介绍和实际操作讲解相结合,全面系统的讲解了 HFSS 天线设计的全过程。是国内最全面、最专业的 HFSS 天线设计课程,可以帮助您快速学习掌握如何使用 HFSS 设计天线,让天线设计不再难...

课程网址: <http://www.edatop.com/peixun/hfss/122.html>

## 13.56MHz NFC/RFID 线圈天线设计培训课程套装

套装包含 4 门视频培训课程,培训将 13.56MHz 线圈天线设计原理和仿真设计实践相结合,全面系统地讲解了 13.56MHz 线圈天线的工作原理、设计方法、设计考量以及使用 HFSS 和 CST 仿真分析线圈天线的具体操作,同时还介绍了 13.56MHz 线圈天线匹配电路的设计和调试。通过该套课程的学习,可以帮助您快速学习掌握 13.56MHz 线圈天线及其匹配电路的原理、设计和调试...

详情浏览: <http://www.edatop.com/peixun/antenna/116.html>



### 我们的课程优势:

- ※ 成立于 2004 年,10 多年丰富的行业经验,
- ※ 一直致力并专注于微波射频和天线设计工程师的培养,更了解该行业对人才的要求
- ※ 经验丰富的一线资深工程师讲授,结合实际工程案例,直观、实用、易学

### 联系我们:

- ※ 易迪拓培训官网: <http://www.edatop.com>
- ※ 微波 EDA 网: <http://www.mweda.com>
- ※ 官方淘宝店: <http://shop36920890.taobao.com>